JST: Engineering and Technology for Sustainable Development
Volume 33, Issue 2, April 2023, 052-059

Influence of the Fixed Angle of the Non-Circular Gears on the Intermediate Shaft on the Gear Ratio Function Characteristics

Nguyen Thanh Trung[1], Phung Van Thom[2*]
[1]National Research Institute of Mechanical Engineering, Ha Noi, Vietnam
[2]Hanoi University of Science and Technology, Ha Noi, Vietnam
[*]Corresponding author email: phungvanthom.hust@gmail.com

Abstract

The paper shows the influence of the fixed angle of non-circular gears (NCGs) on the gear ratio function characteristics of the compound non-circular gear (CNCG) train. The research established a mathematical model describing the centrodes of a typical CNCG train. The fixed angle β of non-circular gears on the intermediate shaft is changed to evaluate its effect on the gear ratio of the CNCG train. The results show that changing the fixed angle of non-circular gears on the intermediate shaft changes the transfer function law of the system and can increase the speed variation range on the output shaft. With the parameters of the designed CNCG train, changing the angle β can increase the amplitude of the gear ratio function to 30.19%. A CNCG train with a speed variation range from 1.37 to 5.11 has been experimentally designed and manufactured with an improved cycloid profile considering the tooth number distribution and satisfying the condition of avoiding undercutting. On that basis, an experimental system to determine the gear ratio of the CNCG train based on the meshing between the gear pairs in the CNCG train has been designed and manufactured. The experimental results showed that the maximum error of the gear ratio function is about 7.63% compared with theoretical ones. In this study, we have not considered the influence of force and torque on the experimental gear ratio. We can apply the results of this research to transmission systems to obtain a speed variation.

Keywords: Compound non-circular gear train, gear ratio function, improved cycloid profile, rack cutter, undercutting.

1. Introduction

Non-circular gear (NCG) trains have the advantage of creating speed and torque converters with a simple mechanical structure, which is increasingly attracting the attention of researchers worldwide. Therefore, more and more scientists are applying non-circular gear transmissions into practice, such as Dawei Liu *et al*. which have used NCG in the design of robot actuators working in the pipeline with the effect of changing the harmonic inertia force and improving the travel efficiency [1]; Wang *et al*. have studied the application of planetary gearbox in automatic rice transplanters [2]. In addition, there are designs in Zhao's automatic transplanters [3]; Thai *et al*. have applied the pair of elliptical gears in the design of the Roots type pump [4, 5]; Prikhodko [6] designed a planetary gear mechanism for the conveyor drive to meet the requirements set forth from practice, etc.

It can be seen that, for the problems of synthesizing NCG transmitters according to the desired transfer function object from practical requirements, most studies on centrodes or complex NCG trains lead to difficulties in synthesizing tooth profiles or the arrangement of pairs of NCG gears. The study of Thai *et al*. [7] has evaluated the influence of centrode design parameters on gear ratio function characteristics. However, there has been no research mentioning that changing the fixed angle of NCGs on the intermediate shaft, while this angle can change the gear ratio function. On the other hand, most of the previous studies used the involutes curve of a circle [8, 9], cycloid [10] or the Novikov-type arc [11] as the tooth profile, or more recently, the involutes curve of ellipse [12].

The disadvantage of the above curves when synthesizing the tooth profile is that the tooth size is often small due to the violation of the condition of undercutting, so it is challenging to perform the problems requiring the large tooth's load capacity. Therefore, the improved cycloid curve [13] is used as the tooth profile to overcome the above disadvantages. In designing the NCGs trains, most studies usually synthesize the centrodes according to a given gear ratio function [14] without paying attention to the gear fixed angle on the intermediate shaft. As a result, centrodes are often complicated curves and do not arrange teeth where the centrode has a small radius of curvature.

ISSN 2734-9381
https://doi.org/10.51316/jst.165.etsd.2023.33.2.8
Received: September 30, 2022; accepted: December 30, 2022

From the problems identified above, in this study, we will evaluate the influence of the fixed angle of the NCGs on the intermediate shaft on the gear ratio function characteristic. The tooth profile of the NCGs trains studied is an improved cycloid [13]. We were solving the problem of tooth number distribution when synthesizing an improved cycloid profile. A compound non-circular gear train is often designed and experimentally fabricated with an improved cycloid profile shaped by a rack cutter to verify the proposed synthesis method. In addition, an experimental system to measure the gear ratio function has been fabricated.

2. Mathematical Model of the Centrodes of the Compound Non-Circular Gear Train

The schematic diagram of the CNCG train is described in Fig. 1.

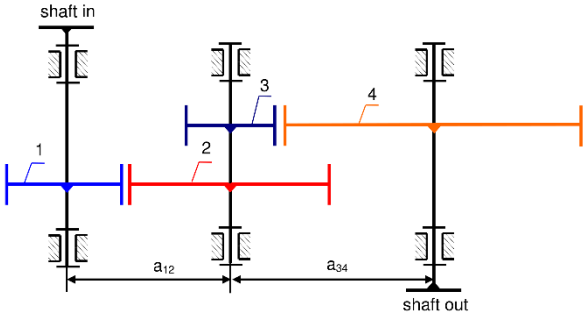

Fig. 1. Schematic diagram of the CNCG train.

wherein:

- Gear 1 is an oval gear whose centrode equation Σ_1 is given by [12]:

$$\rho_1(\phi_1) = \frac{2a_1b_1}{(a_1+b_1)-(a_1-b_1)\cos(2\phi_1)} \tag{1}$$

with: a_1, b_1 are the semi-major and semi-minor axis of Σ_1 and the polar angle $\phi_1 \in [0 \div 2\pi]$ (rad), respectively;

- Gear 3 is an eccentric cylindrical gear whose centrode equation Σ_3 is described by [7]:

$$\rho_3(\phi_3) = \sqrt{R_3^2 - e_3^2 \sin^2\phi_3} + e_3\cos\phi_3 \tag{2}$$

with: R_1, e_1 are the radius of the circle and the eccentricity and the pole angle $\phi_3 \in [0 \div 2\pi]$, respectively.

According to the schematic diagram Fig. 1, gear pairs 1-2 and 3-4 are two pairs of external gears. We have a mathematical equation describing the centrode Σ_2 of the NCG 2 and the centrode Σ_4 of the NCG 4 as follows:

$$\Sigma_2 : \begin{cases} \rho_2(\phi_2(\phi_1)) = \\ \quad a_{12} - \left(\dfrac{2a_1b_1}{(a_1+b_1)-(a_1-b_1)\cos(2\phi_1)}\right) \\ \phi_2(\phi_1) = \\ \quad \displaystyle\int_0^{\phi_1} \left(\frac{2a_1b_1}{a_{12}\left((a_1+b_1)-(a_1-b_1)\cos(2\phi_1)\right)-2a_1b_1}\right) d\phi_1 \end{cases} \tag{3}$$

$$\Sigma_4 : \begin{cases} \rho_4(\phi_4(\phi_3)) = \\ \quad a_{34} - \left(\sqrt{(R_3^2 - e_3^2\sin^2\phi_3)} + e_3\cos\phi_3\right) \\ \phi_4(\phi_3) = \\ \quad \displaystyle\int_0^{\phi_3} \left(\frac{\sqrt{(R_3^2 - e_3^2\sin^2\phi_3)} + e_3\cos\phi_3}{a_{34} - \left(\sqrt{(R_3^2 - e_3^2\sin^2\phi_3)} + e_3\cos\phi_3\right)}\right) d\phi_3 \end{cases} \tag{4}$$

The shaft distance of the NCG pairs is determined by:

$$\begin{cases} a_{12}(a_1,b_1,n_1) = \dfrac{(a_1+b_1)+\sqrt{\left((a_1+b_1)^2 - 4a_1b_1(1-n_1^2)\right)}}{2} \\ a_{34}(n_3,e_3,R_3) = R_3(1+n_3)\left(1-\dfrac{(n_3-12)e_3^2}{4n_3R_3^2}\right) \end{cases} \tag{5}$$

here: n_1 is the number of revolutions for NCG 1 to make one revolution of NCG 2 and n_3 is the number of revolutions for NCG 3 to make one revolution of NCG 4.

3. Effect of the Fixed Angle of the Non-Circular Gears on the Intermediate Shaft on the Gear Ratio Function Characteristics of the Compound Non-Circular Gear Train

3.1. Gear Ratio Function of Compound Non-circular Gear Train

We have the gear ratio function of the CNCG train given by:

$$\begin{cases} i_{12} = \dfrac{\omega_1}{\omega_2} = \dfrac{\rho_1(\phi_1)}{\rho_2(\phi_2(\phi_1))} \\ i_{34} = \dfrac{\omega_3}{\omega_4} = \dfrac{\rho_4(\phi_4(\phi_3))}{\rho_3(\phi_3)} \\ i_{14} = \dfrac{\omega_1}{\omega_4} = i_{12}i_{34} = \left(\dfrac{\rho_1(\phi_1)}{\rho_2(\phi_2(\phi_1))}\right)\left(\dfrac{\rho_4(\phi_4(\phi_3))}{\rho_3(\phi_3)}\right) \end{cases} \tag{6}$$

Substituting (1), (2), (3), and (4) into (6), after the transformation, we have:

$$\begin{cases} i_{12} = \dfrac{\omega_1}{\omega_2} = \dfrac{a_{12}\left((a_1+b_1)-(a_1-b_1)\cos(2\phi_1)\right)}{2a_1b_1} - 1 \\ i_{34} = \dfrac{\omega_3}{\omega_4} = \dfrac{a_{34} - \left(\sqrt{(R_3^2 - e_3^2\sin^2\phi_3)} + e_3\cos\phi_3\right)}{\sqrt{(R_3^2 - e_3^2\sin^2\phi_3)} + e_3\cos\phi_3} \\ i_{14} = \dfrac{\omega_1}{\omega_4} = \left(\dfrac{a_{12}\left((a_1+b_1)-(a_1-b_1)\cos(2\phi_1)\right)}{2a_1b_1} - 1\right) \times \\ \qquad \times \left(\dfrac{a_{34} - \left(\sqrt{(R_3^2 - e_3^2\sin^2\phi_3)} + e_3\cos\phi_3\right)}{\sqrt{(R_3^2 - e_3^2\sin^2\phi_3)} + e_3\cos\phi_3}\right) \end{cases} \quad (7)$$

Since NCG 2 and NCG 3 are fixed on the same axis 2, from (7) we have a relationship between the angular velocity of axes 2 and 3 relative to axis 1:

$$\omega_2 = \frac{2a_1b_1}{a_{12}\left((a_1+b_1)-(a_1-b_1)\cos(2\phi_1)\right) - 2a_1b_1}\omega_1 \quad (8a)$$

$$\omega_4 = \left(\frac{2a_1b_1}{a_{12}\left((a_1+b_1)-(a_1-b_1)\cos(2\phi_1)\right) - 2a_1b_1}\right) \times \times \left(\frac{\sqrt{(R_3^2 - e_3^2\sin^2\phi_3)} + e_3\cos\phi_3}{a_{34} - \left(\sqrt{(R_3^2 - e_3^2\sin^2\phi_3)} + e_3\cos\phi_3\right)}\right)\omega_1 \quad (8b)$$

3.2. Effect of the Fixed Angle of the Non-circular Gears on the Intermediate Shaft on the Gear Ratio Function Characteristics

When changing the fixed angle of the NCG on the input or output shaft, the gear ratio of the CNCG train is changed only in phase angle, but not in value. On the other hand, when changing the fixed angle of the NCG on the intermediate shaft the characteristic of the gear ratio of the CNCG train will be changed in both phase angle and value. To clarify this, with the controdes design parameters of the NCGs of the CNCG train given in Table 1, we evaluate the influence of the fixed angle β of NCG 3 on the intermediate shaft 2 as described in Fig. 2 to the gear ratio characteristic of the CNCG train.

Table 1. The centrodes design parameters of the CNCG train.

Parameter	Notation	Unit	Gear pair 1-2		Gear pair 3-4	
			Oval gear 1	Oval gear 2	NCG 3	NCG 4
The semi-major axis of Σ_1	a	mm	50.0	--	--	--
The semi-minor axis of Σ_1	b	mm	30.0	--	--	--
Circumference coefficient	n	--	1		3	
The radius of Σ_3	R	mm	--	--	25.0	--
The eccentricity of Σ_3	e	mm	--	--	5.0	--
Center distance	a_{12}, a_{34}	mm	80.0		99.0	

Due to the symmetrical nature of NCG 3, we survey the gear ratio in the value domain $\beta = [0 \div 180^\circ]$ with the increment $\Delta\beta = 30^\circ$ and the survey cases described in Table 2.

From the database in Table 1 and Table 2, after solving by numerical calculation on Matlab, Fig. 3 is the survey graph of gear ratio i_{14} of the CNCG train.

Table 2. Fixed angle NCG 3 on axis 2 relative to standard "**0**".

Case	1	2	3	4	5	6	7
β[o]	0	30	60	90	120	150	180

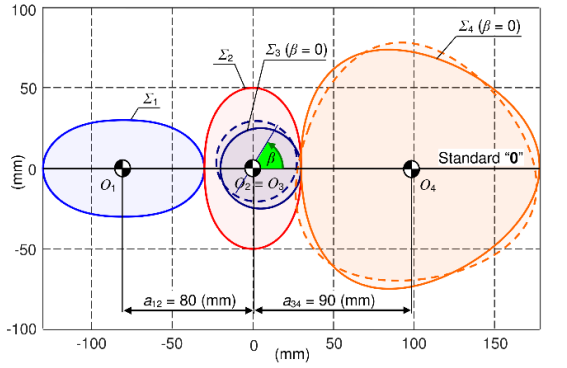

Fig. 2. Position of controdes in the CNCG train

From Fig. 3, it can be seen that when the fixed angle β changes, the gear ratio of the CNCG train will be changed in both geometric shape and amplitude. Moreover, for a more accurate assessment, we call $\delta i_{14}(\beta)$ the amplitude variation of the gear ratio.

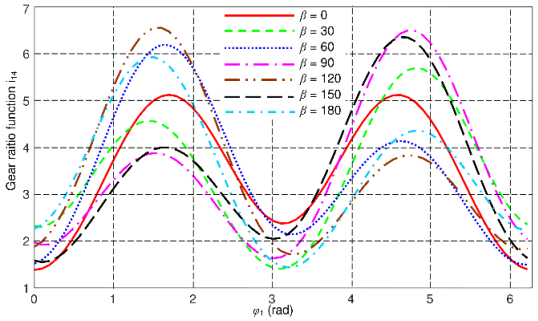

Fig. 3. Gear ratio i_{14} of the CNCG train according to the fixed angle NCG 3 on axis 2.

Then, we have $\delta i_{14}(\beta) = i_{14\max}(\phi_1) - i_{14\min}(\phi_1)$ where $i_{14\max}(\phi_1)$ and $i_{14\min}(\phi_1)$ are the maximum and minimum gear ratios, respectively, and they are determined from the graph in Fig. 3. After calculation, Fig. 4 describes the amplitude $\delta i_{14}(\beta)$ of the gear ratio i_{14} according to the fixed angle β.

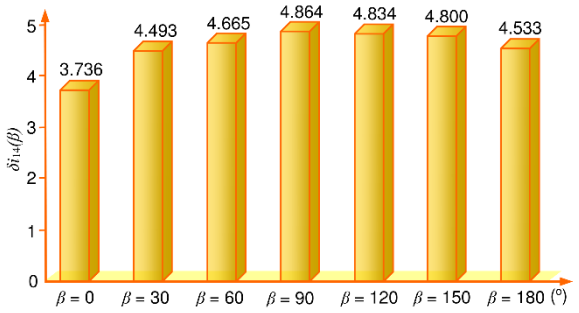

Fig. 4. The amplitude $\delta i_{14}(\beta)$ of the CNCG train according to the fixed angle β.

With centrode design parameters in Table 1, from Fig. 4, we can see that if the fixed angle β increases from 0° to 90° the amplitude of the gear ratio δi_{14} increases, and when the fixed angle β increases from 90° to 180°, the amplitude of the gear ratio decreases, with $\delta i_{14\max|\beta=90^{\circ}} = 4.864$ and $\delta i_{14\min|\beta=0^{\circ}} = 3.736$. Thereby, it is clear that changing the angle β will lead to an increase in the amplitude of the gear ratio function up to 30.19%.

4. Shaping the Tooth Profile of Non-circular Gears by Rack Cutter with an Improved Cycloid Profile

4.1. Mathematical Model of the Rack Cutter

NCGs were shaped by rack cutter with improved cycloid profile as described in Fig. 5 [13], while the mathematical model of the tooth profile Γ_S of the rack cutter is given by following:

$$\mathbf{r}_{K_S} = \begin{bmatrix} x_{K_S} \\ y_{K_S} \\ 0 \end{bmatrix} = \begin{bmatrix} s_2(\phi_S) - a_S \sin(\psi_S) \\ (-1)^g s_3(\phi_S) - a_S \cos(\psi_S) \\ 0 \end{bmatrix} \quad (9)$$

wherein:

$g = 0$ when Γ_S is the addendum profile and $g = 1$ when Γ_S is the dedendum profile of the rack cutter.

and:

$$s_2(\phi_S) = s_1(\phi_S) + r_S(\phi_S)\sin(\psi_S - \phi_S),$$
$$s_3(\phi_S) = r_S(\phi_S)\cos(\psi_S - \phi_S),$$
$$s_1(\phi_S) = \int_0^{\phi_S} \sqrt{r_S(\phi_S)^2 + \left(\frac{dr_S(\phi_S)}{d\phi_S}\right)^2}\, d\phi_S,$$
$$\psi_S = \phi_S + \mu_S - \frac{\pi}{2},$$
$$\mu_S = \tan^{-1}\left(\frac{r_S(\phi_S)}{dr_S / d\phi_S}\right),\ r_S(\phi_S) = a_S\sqrt{\frac{1-\varepsilon^2}{1-\varepsilon^2\cos^2\phi_S}},$$

$\varepsilon = \frac{\sqrt{a_S^2 - b_S^2}}{a_S}$. The parameters a_S, b_S, φ_S are the semi-major, semi-minor, and polar angles of the ellipse generating Σ_S. The machining parameters of the rack cutter are given in Table 3.

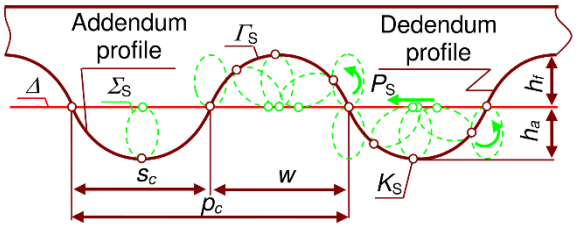

Fig. 5. Rack cutter tooth profile with an improved cycloid curve.

Table 3. Machining parameters of the rack cutter.

Parameter	Notation	Equation
Module	m_c	$m_c = \frac{2\int_0^{2\pi}\sqrt{r_S(\phi_S)^2 + \left(\frac{dr_S(\phi_S)}{d\phi_S}\right)^2}\, d\phi_S}{\pi}$
Tooth thickness on the datum line Δ	s_c	$s_c = \int_0^{2\pi}\sqrt{r_S(\phi_S)^2 + \left(\frac{dr_S(\phi_S)}{d\phi_S}\right)^2}\, d\phi_S$
Width of space on the datum line Δ	w_c	$w_c = \int_0^{2\pi}\sqrt{r_S(\phi_S)^2 + \left(\frac{dr_S(\phi_S)}{d\phi_S}\right)^2}\, d\phi_S$
Tooth pitch on the datum line Δ	p_c	$p_c = 2\int_0^{2\pi}\sqrt{r_S(\phi_S)^2 + \left(\frac{dr_S(\phi_S)}{d\phi_S}\right)^2}\, d\phi_S$
Tooth addendum	h_a	$h_a = 2a_S$
Tooth dedendum	h_f	$h_f = 2a_S$
Whole depth	h	$h = 4a_S$

4.2. Mathematical Model of the Profile of the NCGs Generated by the Rack Cutter

The shaping method was developed in the study [15]. The process of shaping the tooth profile is described in Fig. 6.

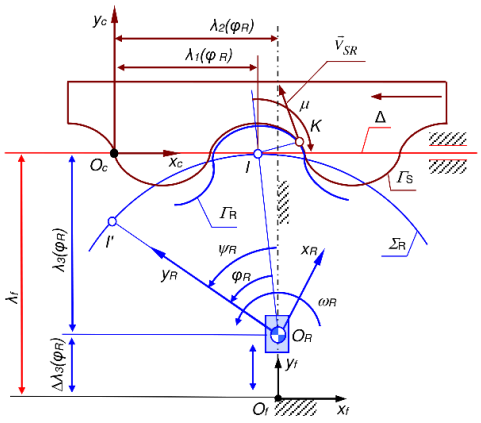

Fig. 6. Illustrating shaping the tooth profile of NCG by the rack cutter.

The mathematical model of the tooth profile shaped by the rack cutter with an improved cycloid profile is given by:

$$\mathbf{r}_{K_R} = \begin{bmatrix} x_{K_R} \\ y_{K_R} \end{bmatrix} = \begin{bmatrix} (\lambda_2(\phi_R) - x_{K_S}(\phi_S))\sin\psi_R(\phi_R) + \\ (\lambda_2(\phi_R) + y_{K_S}(\phi_S))\sin\psi_R(\phi_R) - \\ +(\lambda_3(\phi_R) + y_{K_S}(\phi_S))\cos\psi_R(\phi_R) \\ -(\lambda_3(\phi_R) - x_{K_S}(\phi_S))\cos\psi_R(\phi_R) \end{bmatrix} \quad (10)$$

wherein:

$$\lambda_1(\phi_R) = \int_0^{\phi_R} \sqrt{\rho_R(\phi_R)^2 + \left(\frac{d\rho_1(\phi_R)}{d\phi_R}\right)^2}\, d\phi_R;$$

$$\lambda_2(\phi_R) = \lambda_1(\phi_R) + \rho_R(\phi_R)\sin(\psi_R - \phi_R);$$

$$\lambda_3(\phi_R) = \rho_R(\phi_R)\cos(\psi_R - \phi_R); \qquad \Delta\lambda_3 = \lambda_f - \lambda_3(\phi_R)$$

and: $\psi_R = \phi_R + \mu - \frac{\pi}{2}$; $\mu = \tan^{-1}\left(\frac{\rho_R(\phi_R)}{d\rho_R(\phi_R)/d\phi_R}\right)$ is the tangent angle at the tangent point I of Σ_R to Δ.

In (10) the geometric relationship between φ_S and φ_R is defined by:

$$f(\phi_S, \phi_R) = \\ = y'(\phi_S)y_{K_S}(\phi_S) + x'(\phi_S)\left(\lambda_1(\phi_R) - x_{K_S}(\phi_S)\right) = 0 \quad (11)$$

with: $x'_{K_S}(\phi_S) = \frac{\partial x_{K_S}(\phi_S)}{\partial \phi_S}$, $y'_{K_S}(\phi_S) = \frac{\partial y_{K_S}(\phi_S)}{\partial \phi_S}$.

4.3. Undercutting

In the process of shaping the tooth profile to avoid the undercut, the tooth profile equation of the rack cutter must satisfy following conditions [13]:

$$\begin{cases} \Delta_1 = \begin{vmatrix} \frac{dx_{K_S}(\phi_S)}{d\phi_S} & -V_{SRx} \\ \frac{\partial f(\phi_S)}{\partial \phi_S} & \frac{\partial f(\phi_R)}{\partial \phi_R}\frac{d\phi_R}{dt} \end{vmatrix} \neq 0 \\ \Delta_2 = \begin{vmatrix} \frac{dy_{K_S}(\phi_S)}{d\phi_S} & -V_{SRy} \\ \frac{\partial f(\phi_S)}{\partial \phi_S} & \frac{\partial f(\phi_R)}{\partial \phi_R}\frac{d\phi_R}{dt} \end{vmatrix} \neq 0 \end{cases} \quad (12)$$

wherein V_{SRx}, V_{SRy} are the components of the relative sliding velocity on the tooth profile of the rack and NCG at the shaping point.

4.4. The Tooth Number Distribution

Let p_1 is the tooth pitch of NCG is shaped by rack cutter. Due to the non-slip rolling condition of the average line Δ and Σ_1 in the shaping process, we have:

$$p_1 = p_C = s_1 + w_1 = s_C + w_C = 2C_{\Sigma_S} \quad (13)$$

where s_1, w_1 are the tooth thickness and the width of space on Σ_1, respectively; with $s_1 = w_1$, and $C_{\Sigma_S} = \int_0^{2\pi} \sqrt{r_S(\phi_S)^2 + \left(\frac{dr_S(\phi_S)}{d\phi_S}\right)^2}\, d\phi_S$ is the circumference of Σ_S.

The module m_1 is:

$$m_1 = m_C = \frac{p_1}{\pi} = \frac{p_C}{\pi} = \frac{2C_{\Sigma_S}}{\pi} \quad (14)$$

On the other hand, we have:

$$p_1 = \frac{C_{\Sigma_1}}{z_1} \quad (15)$$

where z_1, C_{Σ_1} are the number of teeth and the centrode circumference of NCG 1, respectively.

From (14) and (15), after transforming we have:

$$z_1 = \frac{C_{\Sigma_1}}{2C_{\Sigma_S}} \quad (16)$$

Let p_2, z_2 and C_{Σ_2} are the tooth pitch, a number of teeth and the circumference of NCG 2, respectively. Non-slip rolling condition of Σ_1 and Σ_2 implies $p_1 = p_2$, then we have:

$$C_{\Sigma_2} = n_1 C_{\Sigma_1} = z_2 p_2 = n_1 z_1 p_1 \quad (17)$$

After simplifying, the number of teeth z_2 of NCG 2 is determined by:

$$z_2 = n_1 z_1 \quad (18)$$

Formula (18) determines the number of teeth of NCG 2 according to the number of teeth of NCG 1 where n_1 is the number of revolutions of NCG1 for NCG 2 to complete one revolution. Therefore, n_1, z_1, and z_2 must be positive integer.

5. Designing the Compound Non-circular Gear Train

From the design data of the centrode of the NCGs in the CNCG train given in Table 1 and the design parameters of the rack in Table 3, with calculating by software written in Matlab, Table 4 is the design data of the rack cutter and Table 5 is the design data of pairs of NCGs. Fig. 7 is the test result of the undercut condition.

Fig. 7 found that the shaped NCGs did not occur undercutting.

After shaping the tooth profile with the data in Table 4 and Table 5, we have the design of pairs of NCGs in the CNCG train as described in Fig. 8 with fixed angular position NCG 3 on the axis taken $\beta = 0^\circ$

To verify that the meshing process between the gear pairs takes place exactly as the theoretical gear

ratio function, we design a speed converter box to serve the measurement of the gear ratio function as described in Fig. 9.

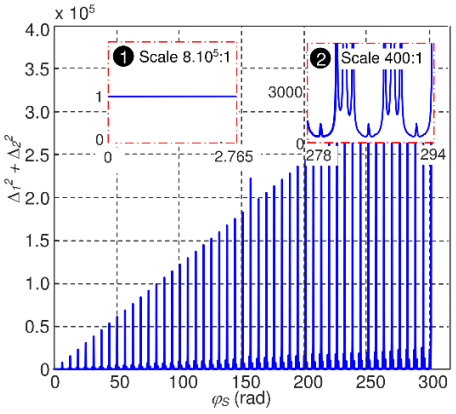

(a)

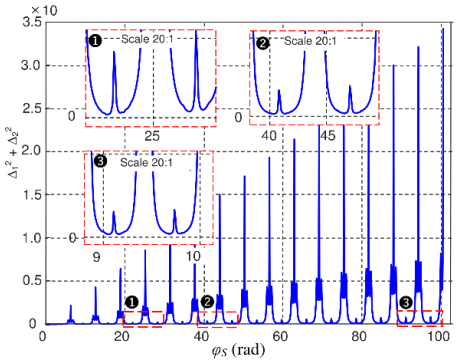

(b)

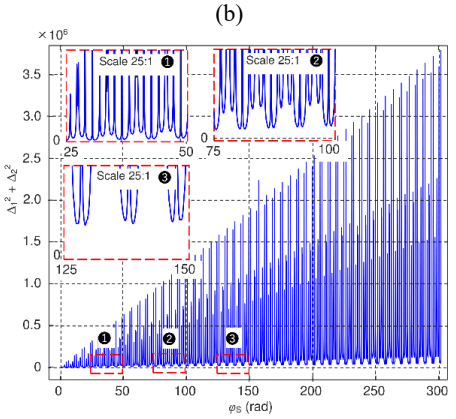

(c)

Fig. 7. Avoidance undercutting occurs with (a) Oval gear, (b) NCG 3 and (c) NCG 4.

Table 4. Design parameters of the rack cutter.

Parameter	Notation	Rack cutter 1	Rack cutter 2
The semi-major axis of Σ_S (mm)	a_S	1.0	1.8
The semi-minor axis of Σ_S (mm)	b_S	0.7	1.4
Module (mm)	m	3.4	6.2
Tooth thickness (mm)	s_c	5.4	9.8
Width of space (mm)	w_c	5.4	9.8
Tooth pitch (mm)	p_c	10.8	19.6
Tooth addendum (mm)	h_a	2.0	3.5
Tooth dedendum (mm)	h_f	2.0	3.5
Whole depth (mm)	h	4.0	7.0

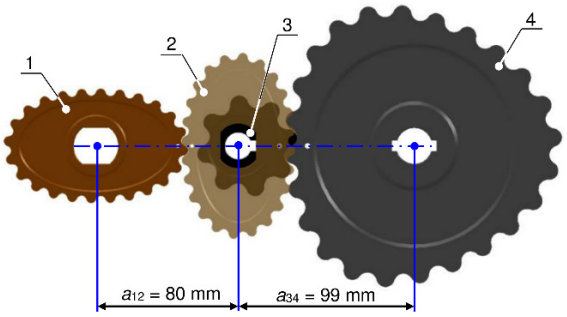

Fig. 8. The design of CNCG.

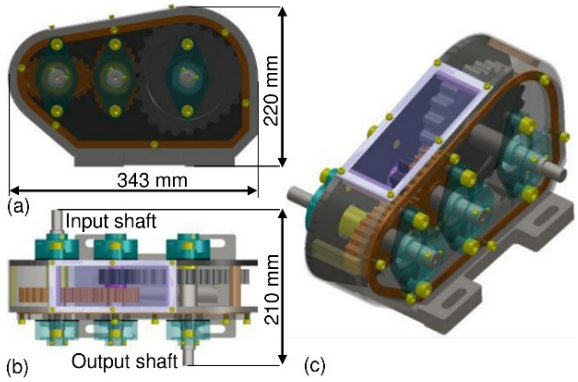

Fig. 9. Speed transform box with (a) Vertical view, (b) Flat view, and (c) 3D Perspective.

Table 5. Design parameters of NCGs.

Parameter	Notation	Gears pair 1-2		Gears pair 3-4	
		Oval gear 1	Oval gear 1	NCG 3	NCG 4
Module (mm)	m	3.4	3.4	6.2	6.2
Circumference coefficient	n	1.0	--	3.0	--
Number of teeth	z	24	24	8	24
Tooth pitch (mm)	p	10.8	10.8	19.6	19.6
Tooth thickness (mm)	s	5.4	5.4	9.8	9.8
Width of space (mm)	w	5.4	5.4	9.8	9.8
Whole depth (mm)	h	4.0	4.0	7.0	7.0
Tooth addendum (mm)	h_a	2.0	2.0	3.5	3.5
Tooth dedendum (mm)	h_f	2.0	2.0	3.5	3.5

6. Experimental Results and Discussion

To determine the gear ratio based on the meshing process between the gear pairs in the CNCG train, with the designed speed transform box, we designed and fabricated an experimental system as described in Fig. 10.

The experimental system consists of a speed transform box with pairs of NCGs arranged as shown in Fig. 9, the input shaft is attached to a Hybrid Servo Motor (86HSE8.5N) through a planetary gear reducer with a gear ratio of 8:1. The rotation speed on the gear shafts is determined independently by the encoders (E6B2-CWZ6C-360 P/R) with a resolution of 360 pulses. The measured data from the encoder is collected by the counter of the PLC (S7-1200, CPU 1214C). An industrial computer (BOXER-6640-A1-1010) as a processing center is used to process data through software written by the authors on TIA Portal V15.1 software. The CNCG train is lubricated by Gadus S2 V220-2 shell grease.

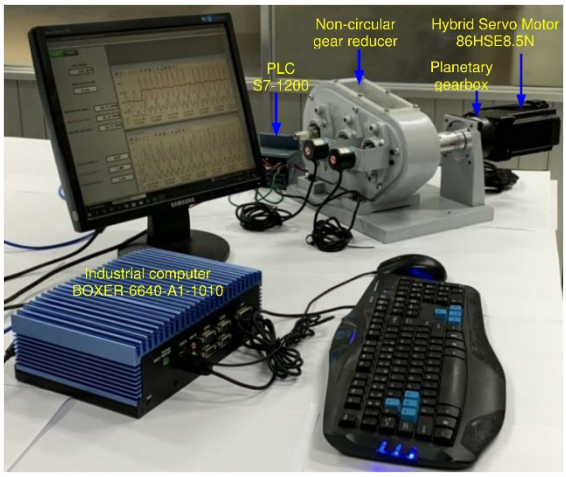

Fig. 10. Experimental system for measuring the transmission ratio function based on the meshing process.

The settings for the data acquisition system is following: sampling period is 0.1 s, the speed set for the Servo motor is 240 rpm, corresponding to the speed of the reducer head attached to the input shaft which is 30 rpm. Fig. 11 shows the results of measuring the gear ratio of pairs of NCGs and the gear ratio of the whole CNCG train with the blue line (rhombus-shaped markers line) being the experimental measurement results and the red line being the gear ratio determined from the centrodes by simulated Matlab.

From the results in Fig. 11, we find that the geometrical shape, the value, and the empirical gear ratio law are approximately the same as the gear ratio function law determined from the centrodes. The largest relative error between theory and experiment occurs at positions 1, 2, and 3, respectively: 2.68%, 6.18%, and 7.63%. Thus, the error on the shaft 3 is the largest, which is caused by the assembly error, in addition to the influence of the inertia force and the resisting moment acting on the output shaft. Since the NCG 4 is mounted on the output shaft and meshes with the NCG 3 is an eccentric cylindrical gear mounted on shaft 2 and shaft 2 is a passive shaft so there is a sudden change in speed. While, in this study, we have not considered the influence of force and torque on the experimental gear ratio.

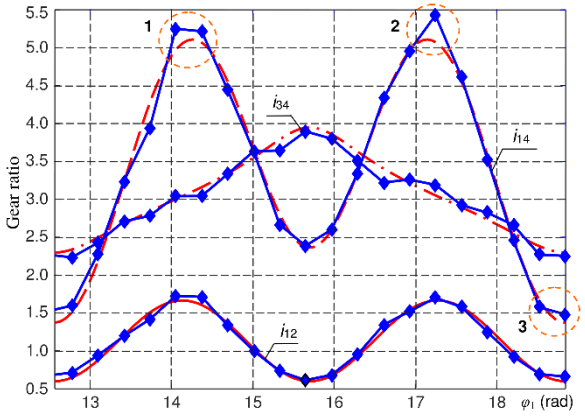

Fig. 11. Graph comparing gear ratio between theory and experiment.

7. Conclusion

From the above theoretical and experimental research results, this study has achieved some main results as follows: (1) Changing the fixed angle of NCGs on the intermediate shaft also changes the gear ratio function, while other studies have to synthesize complex centrodes, and (2) The calculated and experimental results have verified the correctness of the method of synthesizing the CNCG train with the improved cycloid profile.

In addition, these designs can be applied to design NCG transmission according to the characteristics of machines and equipment in practice. However, the limitations of this study are that it does not include issues such as dynamics, power, and performance, and these issues will be part of our future research goals to complete the study.

References

[1] Liu D., Lu J., Cao Y., Jin X., Dynamic characteristics of two-mass impact pipeline robot driven by non-circular gears, Advances in Mechanical Engineering, vol. 14, no. 5, 2022. https://doi.org/10.1177/16878132221095913

[2] Lei Wang, Liang Sun, Hengmin Huang, Yaxin Yu, Gaohong Yu, Design of clamping-pot-type planetary gear train transplanting mechanism for rice wide narrow row planting, Int J Agric & Biol Eng, vol. 14, no. 2, pp. 62 – 71, 2021. https://doi.org/10.25165/j.ijabe.20211402.5975

[3] Xiong Zhao, Hongwei Liao, Xingxiao Ma, Li Dai, Gaohong Yu, Jianneng Chen, Design and experiment of double planet carrier planetary gear flower

transplanting mechanism, Int J Agric & Biol Eng, vol. 14, no. 2, pp. 55 – 61, 2021.
https://doi.org/ 10.25165/j.ijabe.20211402.5878

[4] T. D. Tinh, T. N. Tien, N. H. Thai, Building a mathematical equation for describing volume changes in suction and pumping chambers of an improved type of the roots blower, J. Sci. Technol. Tech. Univ., vol. 141, pp. 022-027 2020.

[5] N. H. Thai, N. D. Long, A new design of the Lobe pump is based on the meshing principle of elliptical gear pairs, Science & Technology Development Journal-Engineering and Technology, vol. 4, no. 2, pp. 861-871, 2021
https://doi.org/10.32508/stdjet.v4i2.769

[6] Prikhodko, Alexander, Dynamic analysis of intermittent-motion conveyor actuator, Actuators, MDPI, vol. 10, no. 8, 2021.
https://doi.org/10.3390/act10080174

[7] N. H. Thai, P. V. Thom, N. T. Trung, Influence of centrodes coefficient on the characteristic of gear ratio function of the compound non-circular gear train with improved cycloid tooth profile, In IFToMM Asian conference on Mechanism and Machine Science, Springer, Cham, 2021, pp. 204-214, 2022. https://doi.org/10.1007/978-3-030-91892-7_19

[8] N. H. Thai, P. V. Thom, Research on the Characteristics of Tooth Shape and Size of the Oval Gear Drive with an Involute Profile, In Regional Conference in Mechanical Manufacturing Engineering, Springer, Singapore, 2022, pp. 167-184.
https://doi.org/10.1007/978-981-19-1968-8_14

[9] Maile Zhou, Yuchao Yang, Mingxu Wei, Daqing Yin, Method for generating non-circular gear with addendum modification and its application in transplanting mechanism, International Journal of Agricultural and Biological Engineering, vol. 13, no.6, pp. 68-75, 2020.
https://doi.org/10.25165/j.ijabe.20201306.5659

[10] Viet, N. H., N. H. Thai, Geometric design and kinematics analysis of non-circular planetary gear train with cycloid profile, Journal of Science and Technology Tech. Univ., vol. 31, no. 3, pp. 105-112, 2021.
https://doi.org/10.51316/jst.151.etsd.2021.31.3.18

[11] N. H. Thai, N. T. Duong, N. H. Viet, Shaping Tooth Profile of Common Non-Circular Gears Using Rack and Novikov Tooth Profile, J. Sci. Technol. Tech. Univ., vol. 140, pp. 011-017, 2020.

[12] N. H. Thai, Shaping the tooth profile of elliptical gear with the involute ellipse curve. Science & Technology Development Journal-Engineering and Technology, vol. 4, no. 3, pp. 1048-1056, 2021.
https://doi.org/10.32508/stdjet.v4i3.820.

[13] N. H. Thai, P. V. Thom, N. T. Trung, Experimental Design and Manufacture a Pair of the Internal Non-circular Gears with an Improved Cycloid Profile, In Regional Conference in Mechanical Manufacturing Engineering, Springer, Singapore, 2022, pp. 118-134. https://doi.org/10.1007/978-981-19-1968-8_11

[14] Fangyan Zheng, Lin Hua, Xinghui Han, Boli, Dingfan Chen, Synthesis of shaped noncircular gear using a three-linkage computer numberial control shaping machine, Journal of Manufacturing Science and Engineering, vol. 139, no. 7, pp. 1 – 12, 2017. https://doi.org/10.1115/1.4035794

[15] Litvin, F. L., Gonzalez-Perez, I., Yukishima, K., Fuentes, A., & Hayasaka, K., Generation of planar and helical elliptical gears by application of rack-cutter, hob, and shaper, Computer methods in applied mechanics and engineering, vol. 196, no. 41-44, pp. 4321-4336, 2007.
https://doi.org/10.1016/j.cma.2007.05.003